Photoinduced Intraensemble Electron Transfer in a Base-Paired Porphyrin−Quinone System. Time-Resolved EPR Spectroscopy

Assia Berman,[†] Elad S. Izraeli,[†] Haim Levanon,*[,†] Bing Wang,[‡] and Jonathan L. Sessler*[,‡]

Contribution from the Department of Physical Chemistry and The Farkas Center for Light-Induced Processes, The Hebrew University of Jerusalem, Jerusalem 91904, Israel, and Department of Chemistry and Biochemistry, The University of Texas, Austin, Texas 78712

Received April 13, 1995[⊗]

Abstract: Recent optical data suggest that porphyrin−guanine (PG) interacts in aprotic solvents with quinone−cytosine (QC) to form a 1:1 donor−acceptor preorganized base-paired supramolecule (PG═QC). To confirm such significant findings, for this novel class of photosynthetic model system, we report here on an independent study by time-resolved electron paramagnetic resonance spectroscopy, combined with selective light excitation. The assemblies (PG═QC) of different porphyrins (zinc−porphyrin, Zn, and free base−porphyrin, H_2) were oriented in liquid crystals of different properties, and the results confirm unambiguously the formation of photoinduced charge-separated states, i.e., $ZnG^{\bullet+}$═$QC^{\bullet-}$ and $H_2G^{\bullet+}$═$QC^{\bullet-}$, with lifetimes of a few microseconds. The unique spin-polarized EPR spectra, which depend on the temperature and solvent, allow the determination of whether the genesis of the electron transfer route is the photoexcited singlet or triplet states of the porphyrin−guanine subunits.

Introduction

The chromophores of the in vivo photosynthetic reaction center are not covalently linked via spacer groups. Rather they are held in space by the protein environment. A novel approach to modeling the primary electron transfer events in photosynthesis involves the synthesis and study of preorganized supramolecular aggregates, containing donors and acceptors which are not covalently linked.[1,2] Along these lines, we recently reported on a study of a porphyrin−quinone electron transfer system (**1**, Figure 1), in which the critical supramoleculer recognition process is established via Watson−Crick base-pairing interactions.[3] Optical measurements of **1** in dichloromethane revealed a fluorescence lifetime of 0.74 ns that was ascribed to the charge-separated state formed as the result of the postulated light-induced, intraensemble electron transfer (IET). Unfortunately, no direct proof of the existence for this charge-separated state and its singlet genesis was provided in this earlier study.[3]

The application of time-resolved electron paramagnetic resonance (TREPR) spectroscopy to the study of IET in photosynthetic model systems is limited by its low time resolution.[4] This is certainly true when IET occurs in molecular ensembles in the liquid phase of isotropic solvents. The main reason for this is the extremely fast electron transfer rates at room temperature (lifetimes are on the order of picoseconds). The problem of low time resolution in TREPR spectroscopy may be dealt with to some extent by modifying the chemical architecture of the donor−acceptor systems. It can also be controlled, often with greater success, by modulating the environmental conditions (e.g., by changing solvent polarity, viscosity, temperature, and medium anisotropy). Within this context liquid crystals (LCs) are of particular interest, since they are known to be convenient media for EPR triplet state detection in the solid and in the fluid nematic phases.[5] In addition and equally important, LCs serve to slow down the rates of intramolecular electron transfer reactions in several donor−spacer−acceptor systems, thus allowing submicrosecond EPR spectroscopic techniques to be applied in the study of these systems.[6,7]

In this study we use liquid crystals to carry out a time-resolved EPR analysis of the IET process that occurs between the

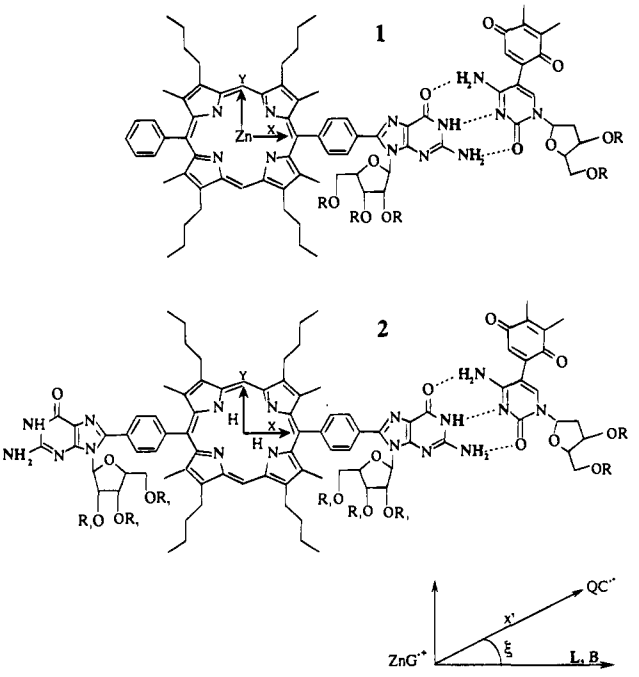

Figure 1. Schematic structures of ZnG═QC (**1**), and H_2G═QC (**2**). R = $SiMe_2Bu^t$. R_1 = isobutyryl. The in-plane axes (*X*, *Y*) of the porphyrin are shown on the molecular structure. The lower scheme represents the frame of reference of the base-paired assembly (see text for details).

[†] The Hebrew University of Jerusalem.
[‡] The University of Texas.
[⊗] Abstract published in *Advance ACS Abstracts,* July 15, 1995.

(1) Turrò, C.; Chang, C. K.; Leroi, G. E.; Cukier, R. I.; Nocera, D. G. *J. Am. Chem. Soc.* **1992**, *114*, 4013.
(2) Tamiaki, H.; Maruyama, K. *Chem. Lett.* **1993**, 1499.
(3) Sessler, J. L.; Wang, B.; Harriman, A. *J. Am. Chem. Soc.* **1993**, *115*, 10418.
(4) Budil, D. E.; Thurnauer, M. C. *Biochim. Biophys. Acta* **1991**, *1057*, 1.
(5) Regev, A.; Galili, T.; Levanon, H. *J. Chem. Phys.* **1991**, *95*, 7907.

0002-7863/95/1517-8252$09.00/0

constituents of **1** and **2**, i.e., Zn–porphyrin–guanine (ZnG) or free-base porphyrin–diguanine (H_2G) and quinone–cytosine (QC) (Figure 1). In comparison, the same experiments were carried out in polar and nonpolar isotropic solvents, and the results confirm the unique solvent behavior of LCs. The results show that different paths of IET processes can be controlled and differentiated by changing the environmental conditions, such as solvent and temperature.

Experimental Section

The synthesis of ZnG, H_2G, and QC was described elsewhere.[3,8] Duroquinone, toluene (Baker analyzed), ethanol (Merck), and LCs (BDH and Merck) were purchased commercially and used without further purification. Direct detection-continuous wave TREPR measurements (200 ns time resolution) were carried out on a Varian E-12 spectrometer. The sample in the microwave cavity was photoexcited at 532 nm by the second harmonic of a Nd:Yag laser (Quanta Ray, DCR-1A) producing 10-ns pulses of 20 mJ/pulse at a repetition rate of 10 Hz.[9] This wavelength corresponds to the Q-band absorption of the porphyrin moiety. All samples, in 4 mm o.d. Pyrex tubes, were degassed by several freeze–pump–thaw cycles on a vacuum line. Alignment of the chromophore–LC samples was carried out according to well-established procedures described elsewhere.[9-11]

Two LCs were used as solvents, E-7 and ZLI-1167.[12] They are typified by different longitudinal dielectric constants ($\epsilon_{||}$) and anisotropic diamagnetic susceptibilities ($\Delta\chi$),[5,13] i.e., $\epsilon_{||} = 19.6$, $\Delta\chi > 0$ and $\epsilon_{||} = 7.5$, $\Delta\chi < 0$, respectively, with the following phase transition temperatures:

$$\text{E-7:}\quad \text{crystalline} \overset{263\ \text{K}}{\leftrightarrow} \text{nematic} \overset{333\ \text{K}}{\leftrightarrow} \text{isotropic} \qquad (1)$$

ZLI-1167:

$$\text{crystalline} \overset{287\ \text{K}}{\leftrightarrow} \text{smectic} \overset{305\ \text{K}}{\leftrightarrow} \text{nematic} \overset{356\ \text{K}}{\leftrightarrow} \text{isotropic} \qquad (2)$$

In the fluid nematic phase of E-7 the director, **L**, is aligned parallel to the external magnetic field, **B** (**L** || **B**), while for ZLI-1167 it is aligned perpendicularly to **B** (**L** ⊥ **B**). These alignments are imposed on the solute chromophore assemblies, embedded in the fluid phases, thereby allowing independent measurements of the electron transfer processes at the two complementary orientations. Based on our previous studies and the results below, the different orientational properties of E-7 and ZLI-1167 (different $\Delta\chi$) are of prime importance in analyzing the electron transfer dynamics by TREPR spectroscopy. On the other hand, the effects of the different dielectric properties ($\epsilon_{||}$) are less apparent in this type of study.

Triplet line shape analysis was preformed by using the density matrix formalism, as described in detail elsewhere.[5,14] The line-shape analysis associated with radical pair spectra was carried out by taking into account the relevant electron spin polarization mechanism.[15,16] The line-shape simulations provided the following data: (1) the zero field splitting (ZFS) parameters of the photoexcited triplet state, $|D|$ and $|E|$; (2) the triplet ← singlet spin–orbit intersystem crossing (SO-ISC) population rate ratios (A_X:A_Y:A_Z); (3) the *g*-factors of the photogenerated doublet radicals; and (4) the relative alignment of the porphyrin canonical axes with respect to **L**.

Analysis of the magnetization, $M_y(t)$, behavior was carried out by using a previously derived biexponential expression:[17]

$$M_y(t) = \omega_1 \frac{[e^{-c_- t} - e^{-c_+ t}]}{c_- - c_+}$$

$$c_\pm = \frac{T_2^{-1} + T_1^{-1}}{2} \mp \left[\frac{(T_2^{-1} - T_1^{-1})^2}{4} - \omega_1^2\right]^{1/2} \qquad (3)$$

where ω_1 is the microwave field and $T_{1,2}$ are the relaxation times.

Results and Discussions

Isotropic Solvents. Photoexcitation of a frozen solution of ZnG (monomer) in toluene gives rise to a conventional triplet EPR spectrum, attributed to the porphyrin constituent ^{3}*ZnG,[9] which is formed via the SO-ISC mechanism. When QC is added to a ZnG solution, in a 1:1 ratio, no photoinduced EPR signal could be observed over a wide temperature range, e.g., between 130 and 298 K. We attribute this effect to the formation of the supramolecule **1**, in which a fast IET process is induced. Replacing toluene by a protic solvent (ethanol), which competes for hydrogen-bonding sites,[3] restores the triplet spectrum of ZnG in the frozen solution (Figure 2).

To check to what extent ZnG and QC are indeed separated species in ethanol, the same experiments were preformed at temperatures above the melting point of ethanol. At these temperatures, molecular diffusion is not restricted, thus allowing the photoinduced intermolecular electron transfer process to occur, i.e.:

$$\text{ZnG} \xrightarrow{h\nu} {}^1\text{*ZnG} \xrightarrow{\text{ISC}} {}^3\text{*ZnG} \qquad (4)$$

$${}^3\text{*ZnG} + \text{QC} \xrightarrow{\text{ET}} \text{ZnG}^{\bullet+} + \text{QC}^{\bullet-} \qquad (5)$$

Thus, encounters and re-encounters of the separated radical ions enable the electron spin polarization processes to develop. The TREPR spectrum of $QC^{\bullet-}$ (Figure 3) reveals a low-field signal emission (e) and high-field absorption (a) pattern, e/a. The attachment of the amino base to the quinone causes an inhomogeneous broadening, which affects the hyperfine structure, an effect that was noticed in other bulky systems consisting of a quinone attached to a protein,[18] or to a porphyrin amide.[7]

In order to estimate the *g*-factor of $ZnG^{\bullet+}$ and to examine the putative electron spin polarization mechanisms involved in this electron transfer process, we studied the reaction of ZnG with a well-known acceptor, e.g., duroquinone. The resulting spectrum, of the duroquinone radical anion, is shown in Figure 3b, along with a simulated spectrum, determined by taking into account two CIDEP mechanisms, namely the triplet mechanism (TM) and the radical pair mechanism (RPM),[15] and using the known *g*-factor of the duroquinone radical anion, 2.0049.[19] The resulting *g*-factor of 2.0038 for $ZnG^{\bullet+}$ is larger then that for $ZnTPP^{\bullet+}$,[20] and smaller than that for the zinc octaethyltetraphenylporphyrin cation radical.[21] Artificial line broadening of the simulated spectrum shown in Figure 3c results in a line shape

(6) Hasharoni, K.; Levanon, H.; von Gersdorff, J.; Kurreck, H.; Möbius, K. *J. Chem. Phys.* **1993**, *98*, 2916.
(7) Hasharoni, K.; Levanon, H.; Gätschmann, J.; Schubert, H.; Kurreck, H.; Möbius, K. *J. Phys. Chem.* **1995**, *99*, 7514.
(8) Sessler, J. L.; Wang, B.; Harriman, A. *J. Am. Chem. Soc.* **1995**, *117*, 704.
(9) Gonen, O.; Levanon, H. *J. Phys. Chem.* **1985**, *89*, 1637.
(10) Levanon, H. *Rev. Chem. Intermed.* **1987**, *8*, 287.
(11) Regev, A.; Levanon, H.; Murai, T.; Sessler, J. L. *J. Chem. Phys.* **1990**, *92*, 4718.
(12) The chemical compositions are as follows: E-7 is an eutectic mixture of R_i–C_6H_5–C_6H_5–CN: R_1= C_5H_{11} (51%); R_2 = C_7H_{15} (25%); R_3 = $C_8H_{17}O$ (16%); R_4 = $C_5H_{11}C_6H_5$ (8%). ZLI-1167 is an eutectic mixture of R'_i–C_6H_{10}–C_6H_{10}–CN: R'_1 = C_3H_7; R'_2 = C_5H_{11}; R'_3 = C_7H_{15}.
(13) Regev, A. Ph.D. Dissertation, Hebrew University of Jerusalem, Jerusalem, 1992.
(14) Gonen, O.; Levanon, H. *J. Phys. Chem.* **1984**, *88*, 4223.
(15) Salikhov, K. M.; Molin, Y. N.; Segdeev, R. Z.; Buchachenko, A. L. *Spin Polarization and Magnetic Effects in Radical Reactions*; Elsevier: Amsterdam, 1984.
(16) Hore, P. J. In *Advanced EPR. Applications in biology and biochemistry*; Hoff, A. J., Ed.; Elsevier: Amsterdam, 1989; pp 405–440.
(17) Hore, P. J.; McLauchlan, K. A. *J. Magn. Reson.* **1979**, *36*, 129.
(18) Ehrenberg, A. *Ark. Kemi* **1962**, *19*, 97.
(19) Landolt-Börnstein. *New Series, Group 12*; Springer-Verlag: Berlin, 1980; Vol. 9.
(20) Bowman, M. K.; Toporowicz, M.; Norris, J. R.; Michalski, T. J.; Angerhofer, A.; Levanon, H. *Isr. J. Chem.* **1988**, *28*, 215.
(21) Unpublished Results.

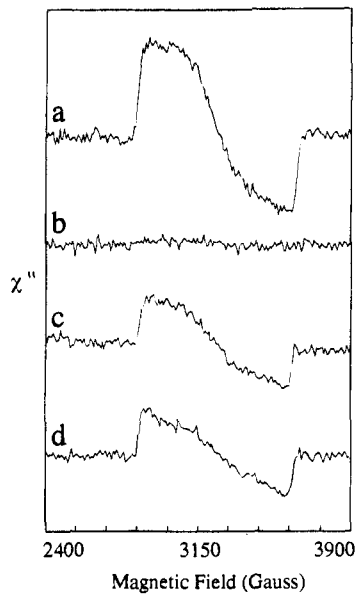

Figure 2. Triplet TREPR spectra of (a) ZnG in toluene; (b) a 1:1 mixture of ZnG and QC in toluene; (c) ZnG in ethanol; and (d) a 1:1 mixture of ZnG and QC in ethanol. The delay time between laser excitation and EPR detection, τ_d, is 350 ns. The temperature is 140 K, and the microwave power is 50 mW.

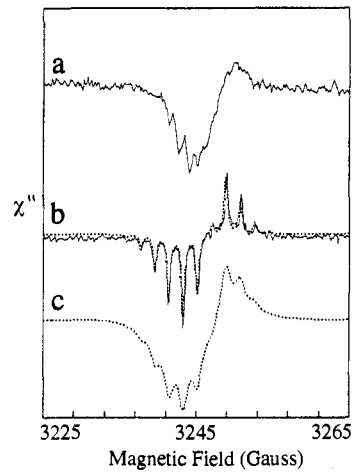

Figure 3. TREPR spectra of a 1:1 mixture in ethanol of (a) ZnG and QC and (b) ZnG and duroquinone. The spectra were taken at $\tau_d = 1$ μs, 243 K, and a microwave power of 10 mW. Simulation of the polarized spectrum of the duroquinone radical anion (dotted line) was carried out by taking into account two electron spin polarization mechanisms: TM and S-T_0 RPM (for details see ref 20). Trace c was obtained by increasing the line width of the simulated spectrum in trace b.

pattern similar to that of $QC^{\bullet -}$. Therefore, we deduce that the mechanisms associated with the intermolecular electron transfer process (reaction 5) are the same as that with duroquinone as an acceptor. In contradistinction to what is observed in ethanol, there is no direct evidence for IET in toluene under conditions where **1** is believed to be formed. We attribute this to the quenching of the porphyrin singlet via fast IET, to produce a short-lived charge-separated radical pair, which escapes EPR detection. The fast IET, which competes with SO-ISC, prevents EPR detection of the triplet state, ^{3}*ZnG—QC, in the solid phase as well. By switching to the anisotropic LC solvent, the IET rates (forward and backward) could be attenuated,[22] thus allowing TREPR detection of several intermediates, which are involved in the IET process.

(22) Hasharoni, K.; Levanon, H. *J. Phys. Chem.* **1995**, *99*, 4875.

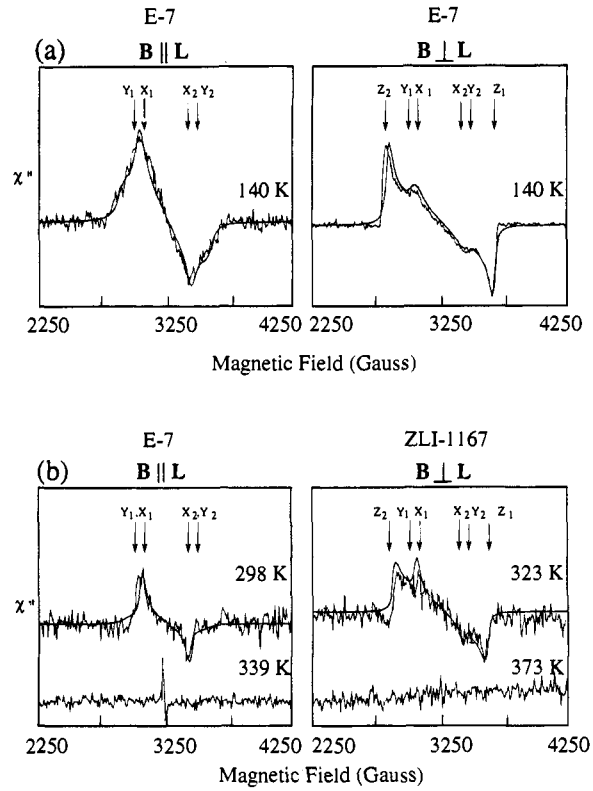

Figure 4. Triplet TREPR spectra of ^{3}*ZnG—QC aligned in E-7 and ZLI-1167. Spectra were taken at $\tau_d = 300$ ns and a microwave power of 50 mW: (a) spectra taken in frozen E-7 at two orientations of the director with respect to the magnetic field; (b) spectra taken in the fluid nematic (upper traces) and isotropic (lower traces) phase of the two indicated LCs. The line shape in the isotropic phase is discussed separately in Figure 6. The solid lines are simulation curves of the triplet spectra: (a) in frozen matrices; (b) in the nematic phase, taking into account triplet dynamics (for details see ref 11).

Liquid Crystals. In Figures 4–6 we show the TREPR spectra of a 1:1 mixture of ZnG (or H_2G) and QC oriented in the nematic and isotropic phases of two different LCs (E-7 and ZLI-1167). It is evident that the spectra are completely different from those recorded in either ethanol or toluene. As will be shown below, the experimental spectra are assigned to the base-paired supramolecule, **1** and **2**. The broad spectra displayed in Figures 4 and 5 (2000 G field sweep) are attributed to the triplets, localized on the porphyrin entities, ^{3}*ZnG—QC and ^{3}*H_2G—QC, while the narrow spectra shown in detail in Figure 6 (40 G field sweep) are attributed to the charge-separated state, $ZnG^{\bullet +}$—$QC^{\bullet -}$ and $H_2G^{\bullet +}$—$QC^{\bullet -}$.

First, we examine the line shapes of the triplet spectra of photoexcited **1** and **2** in the crystalline phase of E-7 (Figures 4a and 5a). The low-temperature spectra (140 K) were obtained at two different orientations of the director, **L**, with respect to the magnetic field **B**, i.e., **L** || **B** and **L** ⊥ **B**. Following the treatment of Regev et al.,[5] the line-shape simulations allow one to assign the canonical axes, *X* and *Y* of the two triplets, ^{3}*ZnG—QC and ^{3}*H_2G—QC (see Figure 1). In the porphyrin frame of reference for both assemblies, the *X*-axes are almost parallel to **L**, with the calculated fluctuation angles, between the in-plane X-axes and **L**, ϕ_0, being equal to 10° and 5°, respectively.[14] The polarization patterns from low to high field are as follows: *a,a,a,e,e,e* and *e,e,e,a,a,a* with A_X:A_Y:A_Z = 0.0:0.5:1.0 and 0.6:1.0:0.0 for ^{3}*ZnG—QC and ^{3}*H_2G—QC, respectively. These patterns are in agreement with those found for the respective tetraphenylporphyrin (TPP) monomers, where the ZnTPP exhibits an out-of-plane spin polarization (*Z*-

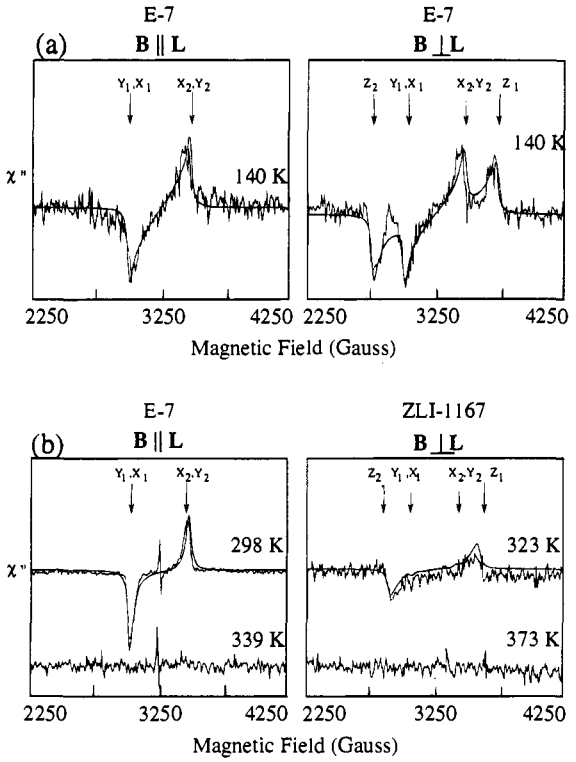

Figure 5. Triplet TREPR spectra of $^{3*}H_2G$–QC aligned in E-7 and ZLI-1167. The spectra were taken at $\tau_d = 600$ ns. Other experimental conditions are as in Figure 4.

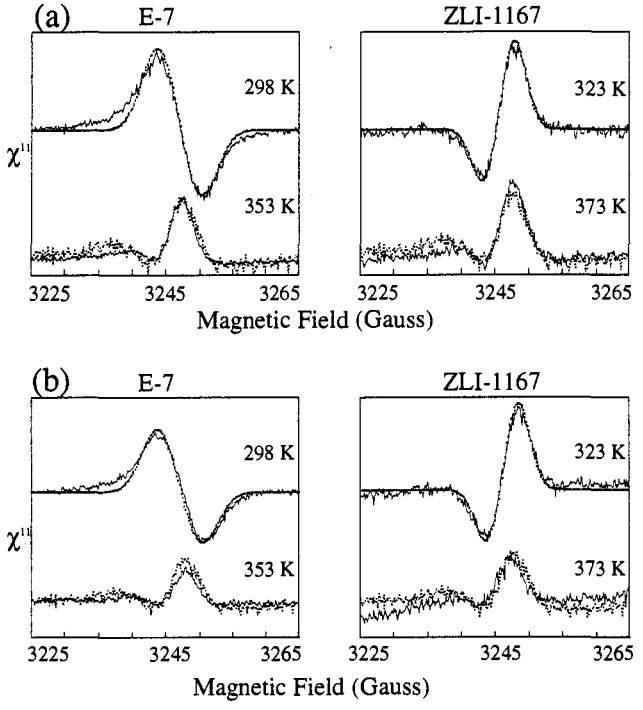

Figure 6. TREPR spectra of (a) $ZnG^{\bullet+}$–$QC^{\bullet-}$; (b) $H_2G^{\bullet+}$–$QC^{\bullet-}$ dissolved in two LCs (E-7, $\Delta\chi > 0$ and ZLI-1167, $\Delta\chi < 0$) at typical nematic and isotropic temperatures. The spectra were taken at τ_d = 900 ns and 50 mW microwave power. The simulations (dotted line) were obtained by employing eq 7 with a Gaussian line shape.

state is selectively populated), while H_2TPP exhibits an in-plane spin polarization (*X*- and *Y*-states are selectively populated).[9,13]

Upon approaching the fluid nematic phase, the LC dynamics start to govern the line shape of the TREPR spectra. In E-7 ($\Delta\chi > 0$), the triplet spectra are characterized by **L** || **B**, where

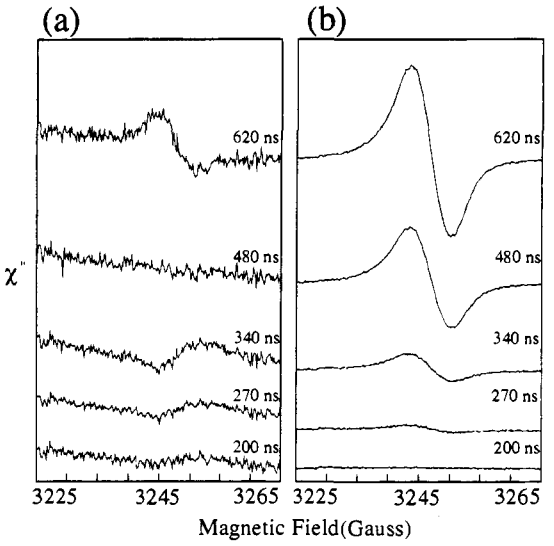

Figure 7. TREPR spectra of $ZnG^{\bullet+}$–$QC^{\bullet-}$ in E-7, at different τ_d. The spectra were recorded at two different phase temperatures: (a) 243 K (soft crystalline phase) and (b) 298 K (nematic phase). All experimental conditions are as in Figure 6.

the long molecular axis (the canonical orientation *X*) is parallel to both **L** and **B**. In ZLI-1167 ($\Delta\chi < 0$), *X* it is also parallel to **L**, but in this LC the orientation is such that **L** ⊥ **B**, which is equivalent to the rotation of the sample tube by $\pi/2$, in the solid phase of E-7 ($\Delta\chi > 0$).[5] Thus, in the $\Delta\chi > 0$ case, the *X*-axis dominates the TREPR spectrum, while in the $\Delta\chi < 0$ case, the *Z* and *Y* canonical axes should dominate, as is indeed confirmed by the experiment (cf. Figures 4b and 5b). The simulation of the triplet spectra in the fluid nematic phase takes into account the molecular dynamics,[5] where the only effective motion is associated with rotation of **1** and **2** about the long *X*-axis (*X* is always parallel to the director, **L**). The rotation rates were found to be 9×10^7 and 1.5×10^7 s^{-1} for $^{3*}ZnG$–QC and $^{3*}H_2G$–QC, respectively. These values are in line with those found for conventional porphyrins.[11] In the isotropic phase both triplets, as expected, escape EPR detection.

We focus now on the narrow polarized spectra, which are characterized by their unique line shapes and attributed to the charge-separated radical pairs. In Figure 7 we show the TREPR spectra of $ZnG^{\bullet+}$–$QC^{\bullet-}$ in the soft-crystalline phase at 243 K and in the nematic phase at 298 K of E-7. At 243 K, the spectrum exhibits a line phase inversion, i.e., at early times (τ < 480 ns), the polarization exhibits an e/a pattern, while at later times the opposite pattern (a/e) is detected. Attempts to detect a spectrum attributed to $H_2G^{\bullet+}$–$QC^{\bullet-}$ in the soft crystalline region failed, while in the nematic and isotropic fluid phases, the spectra are similar to those of $ZnG^{\bullet+}$–$QC^{\bullet-}$, exhibiting the same polarization patterns.

To assign a specific mechanism that explains the line shape behavior, we examined the spectra of the charge-separated state at elevated temperatures, in the nematic phase, where line phase inversion was not detected. In Figure 6 we present the TREPR spectra of **1** and **2** in the two LCs. Similar to the broad triplets, which depend on the specific LC solvent, the line shapes of the radical pair signals were also found to be dependent on the LC properties, i.e., $\Delta\chi$. It is evident that the polarization pattern from low to high field is a/e in E-7 and e/a in ZLI-1167. These patterns were not changed over the entire temperature range of the nematic phase. They are different from those shown in Figure 3, which arise from $QC^{\bullet-}$ in ethanol.

Another possible assignment of the radical pair spectra is through the IET reaction to produce the triplet radical pair:

$$[^3*P\text{···}QC] \rightarrow {}^3[P^{\bullet+}\text{···}QC^{\bullet-}] \quad (6)$$

where P stands for ZnG or H_2G. However, this mechanism is ruled out since the EPR line shapes of **1** and **2** are almost identical (Figure 6). This consideration is based on the fact that the line shape of the $^3[P^{\bullet+}\text{···}QC^{\bullet-}]$ is governed by the triplet polarization transfer process, as outlined in reaction 6.[6] In other words, the out-of-plane selective population of ^{3*}ZnG···QC, as compared to the in-plane selective population of $^{3*}H_2G$···QC, should result in different triplet radical-pair spectra, contrary to the spectra observed here, independent of the triplet precursor.

Ruling out the formation of the $^3[P^{\bullet+}\text{···}QC^{\bullet-}]$ state can also come from an examination of the kinetic traces in Figure 8. These traces were taken for **1** and **2** in the nematic phase of E-7 at different temperatures. It is apparent that while the kinetics of the product formation via the IET (traces b in Figure 8) are almost identical for the two photoexcited assemblies, the kinetics and phases of the triplet magnetization are different (traces a in Figure 8). From eq 3, the triplet magnetization decay times were calculated to be ~0.1 μs for ^{3*}ZnG···QC and ~0.3 μs for $^{3*}H_2G$···QC, almost identical with those of ZnG and H_2G monomers in E-7 (data not shown). Moreover, for reaction 6 to occur, the rise time of the IET product (>0.5 μs) should be correlated with the magnetization decay time of the triplet. In our case there is no such correlation; the magnetization rise and decay rates of the IET product increase with temperature, whereas the rates of the triplet almost do not change with temperature. The different triplet kinetic traces (a in Figure 8) explain clearly why the triplet and radical pair spectra of **1** cannot be detected simultaneously (Figure 4b), while those of **2** are easily detected (Figure 5b).

The polarization mechanism that may account for the experimental derivative-like spectra involves a correlated radical pair mechanism (CRPM).[23-25] The different polarization patterns in E-7 and ZLI-1167, i.e., a/e vs e/a (Figure 6), are consistent with such a CRPM, in which the peak-to-peak separation (ΔB) of the spectrum is expressed in terms of the exchange and dipolar interactions, J and D, respectively, through the following relation:[16]

$$\Delta B = |2[J - D(\cos^2\theta - \tfrac{1}{3})]| \quad (7)$$

where θ is the angle between the dipolar axis, x', and the external magnetic field, **B**. Simulation of the experimental spectra that describes the radical pair states of ($ZnG^{\bullet+}\text{···}QC^{\bullet-}$) and ($H_2G^{\bullet+}\text{···}QC^{\bullet-}$), taken in the two LCs, was carried out by considering the alignment properties of the two LCs. For E-7 ($\Delta B_{B\|L}$), $\theta = \xi$, and for ZLI-1167 ($\Delta B_{B\perp L}$), $\theta = \xi + \pi/2$, where ξ is the angle between the dipolar axis, x', and **L** (Figure 1). The dependence of ΔB on θ explains the different peak-to-peak separations in the two different LCs. By using the point-dipole approximation, with a center-to-center distance of ~15 Å,[26] the dipolar interaction, D, was calculated to be -7×10^{-4} cm^{-1}. The negative sign is due to the head-to-tail spin alignment.[27] Assuming $J < 0$ and from eq 7, its value was calculated to be

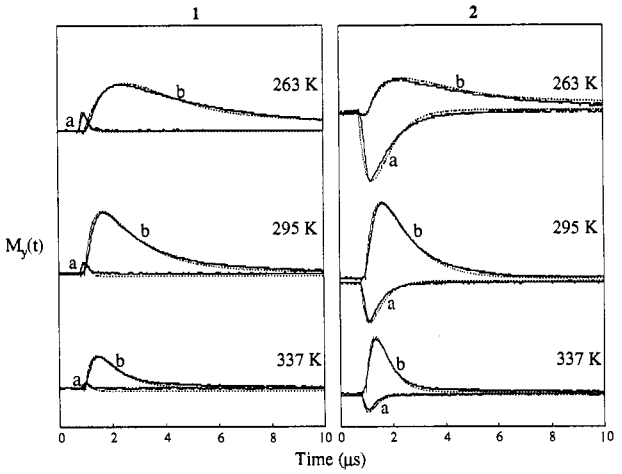

Figure 8. (a) Triplet magnetization traces, at three temperatures in the nematic phase of E-7, taken at field positions Z_2 for **1** and X_1 for **2**, shown in Figures 4 and 5, respectively. The different phases reflect the different population routes of the two triplets; (b) formation and decay curves of the radical pair magnetization.

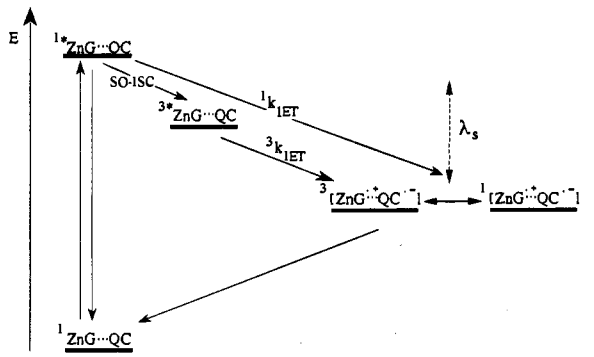

Figure 9. Schematic energy level diagram for the different IET paths discussed in the text. The vertical dashed arrow is meant to depict the tunability of the charge-separated state via the reorganization energy, λ_s.

~-9×10^{-5} cm^{-1}, and that of ξ ~25° in agreement with the calculated structure of **1**.[26]

In principle, the precursor state that initiates the IET can be either the photoexcited singlet or triplet state of the porphyrin. This can be determined by the experimental polarization pattern via the correlated radical pair sign rule:[16]

$$\Gamma = -\mu \sin[J + D(3\cos^2(\theta) - 1)] = \begin{cases} -e/a \\ +a/e \end{cases} \quad (8)$$

the sign of μ determines whether the IET is a singlet- or a triplet-initiated process, i.e., (−) or (+), respectively. By inserting the values of J, D, and θ into eq 8, we get $\mu = +$ (triplet precursor) for the a/e spectrum ($\Gamma_{B\|L} = +$) and $\mu = +$ (again, a triplet precursor) for the e/a spectrum ($\Gamma_{B\perp L} = -$).

As mentioned earlier, a signal phase inversion in the correlated radical pair spectra (Figure 7) is noticed in the soft crystalline region of E-7 (243 K). This observation does not contradict the conclusion that the triplet precursor governs the correlated radical pair spectra in the fluid phase of the LCs. Since the field position of the inverted lines is the same, we may assume that they describe the same radical pair state. In other words, a competition between the singlet-initiated radical pair and the ISC rate (to produce the triplet precursor of the radical pair) should be considered in determining the phase of the spectrum. In more detail, let us consider Figure 9, as it would appear with two limiting cases: (1) the charge-separated state lies above the triplet state of the porphyrin donor, thus

(23) Buckley, C. D.; Hunter, D. A.; Hore, P. J.; McLauchlan, K. A. *Chem. Phys. Lett.* **1987**, *135*, 307.
(24) Closs, G. L.; Forbes, M. D. E.; Norris, J. R. *J. Phys. Chem.* **1987**, *91*, 3592.
(25) Norris, J. R.; Morris, A. L.; Thurnauer, M. C.; Tang, J. *J. Chem. Phys.* **1990**, *92*, 4239.
(26) Geometry optimization of **1** was preformed by molecular mechanics, MM+ force field calculation, preformed by Hyperchem software (Autodesk Inc.).
(27) Levanon, H.; Norris, J. R. *Chem. Rev.* **1978**, *78*, 185.

the IET process occurs exclusively via the singlet route; (2) the charge-separated state lies below the triplet state of the porphyrin donor, thus the IET process can occur concurrently through the singlet and triplet routes (to create the correlated radical pair signal). These two extreme cases are differentiated in terms of the reorganization energy, λ_s, a parameter that is a function of the solvent characteristics.[7,28]

The experimental reality actually lies somewhere between these two limiting cases. At low temperatures, in the solid phase of E-7, only the triplet states ^{3*}ZnG···QC (and $^{3*}H_2G$···QC) are EPR detected, whereas in the less polar LC, ZLI-1167, an extremely weak correlated radical pair spectrum (singlet initiated) can be detected (data not shown). This implies that in both LCs the charge-separated state lies above the triplet state. Increasing the temperature and moving into the soft crystalline regime of the LCs makes solvent reorganization more facile. This then makes the charge-separated state readily attainable via the singlet and triplet routes, thus a phase inversion of the TREPR signal is expected. At early times the singlet-initiated route predominates, while at later times the triplet route takes over, as indicated by the phase inversion of the correlated radical pair signal (Figure 7). Increasing the temperature further, brings the LCs into their nematic fluid phase. This results in a further decrease in the energy of the charge-separated state, and in this case the triplet-initiated route dominates. The observation is contrary to what is found with covalently linked donor–spacer–acceptor systems, characterized by fixed distances.[6] In the present case, however, the intermolecular distances in the hydrogen-bonded complexes, ZnG···QC (or H_2G···QC), are more flexible, and are expected to be temperature dependent. This may result in some alternation in the activation energy of the IET process and thus could end up shifting (at high temperatures) a singlet-initiated route into a triplet-initiated one, as has been previously observed in the case of an electrostatically-bound donor–acceptor system.[29]

(28) Lendzian, F.; von Maltzan, B. *Chem. Phys. Lett.* **1991**, *180*, 191.

In the isotropic liquid phase, which is above the clearing point of the LCs, the triplet state, as expected, escapes EPR detection,[30] while the EPR signal of the radical pair is clearly detected. The polarized spectra in both LCs exhibit the same width and phase pattern, namely a weak emission at low field and a strong absorption at high field. Here the relevant signal could be simulated by adding together the two spectra, taken in the nematic phase at $\mathbf{B} \parallel \mathbf{L}$ and $\mathbf{B} \perp \mathbf{L}$, with a ratio of 1:2, respectively (Figure 6).[31]

The results reported in this paper serve to illustrate the straightforward correlation between spin dynamic analyses, for instance presented here, and optical spectroscopy measurements[3] in studying IET processes. In particular, this paper focuses on a novel donor–acceptor system and not only provides a further characterization of this prototypical non-covalent photosynthetic model system but also serves to highlight how solvent properties and TREPR spectroscopy are linked together in IET studies.

Acknowledgment. We are grateful to Mrs. T. Galili for her kind assistance. This work was supported by the U.S.–Israel Binational Science Foundation, the Deutsche Forschungsgemeinschaft (Sfb 337), the Volkswagen Stiftung (H.L.), and The Robert A. Welch Foundation (F-1018) and the National Institutes of Health (GM 41657) (J.L.S.). The Farkas Research Center is supported by the Bundesministerium für die Forschung und Technologie and the Minerva Gesellschaft für Forschung GmbH, FRG. This work is in partial fulfillment of the requirements for a Ph.D. degree (A.B) and M.Sc. (E.I) at the Hebrew University of Jerusalem.

JA951259Y

(29) Zilber, G.; Rozenshtein, V.; Levanon, H.; Rabinovitz, M. *Chem. Phys. Lett.* **1992**, *196*, 255.

(30) Weissman, S. I. *J. Chem. Phys.* **1958**, *29*, 1189.

(31) The two LCs differ in their solvent properties, e.g., dielectric constant, viscosity, light transmission, alignment, etc. Therefore, the experimental ratio of 1:2 in reconstructing the isotropic spectra is qualitative.